From nanohelices to magnetically actuated microdrills: a universal platform for some of the smallest untethered microrobotic systems for low Reynolds number and biological environments

Tian Qiu [1, 2], John G. Gibbs [1], Debora Schamel [1, 3], Andrew G. Mark [1], Udit Choudhury [1], and Peer Fischer [1, 3]

[1] Max Planck Institute for Intelligent Systems, 70569 Stuttgart, Germany
[2] Institute of Bioengineering, Ecole Polytechnique Fédérale de Lausanne (EPFL), CH-1015 Lausanne, Switzerland
[3] Institut für Physikalische Chemie, Universität Stuttgart, Pfaffenwaldring 55, 70569 Stuttgart, Germany
fischer@is.mpg.de

Abstract. Building, powering, and operating structures that can navigate complex fluidic environments at the sub-mm scale are challenging. We discuss some of the limitations encountered when translating actuation mechanisms and design-concepts from the macro- to the micro-scale. The helical screw-propeller or drill is a particularly useful geometry at small scales and Reynolds numbers, and is one of the mechanisms employed by microorganisms to swim. The shape necessarily requires three-dimensional fabrication capabilities which become progressively more challenging for smaller sizes. Here, we report our work in building and operating these screw-propellers at different sizes. We cover the length scales from the sub 100 nm to drills that are a few hundred microns in length. We use a known physical deposition method to grow micron-sized magnetic propellers that we can transfer to solutions. We have recently succeeded in extending the fabrication scheme to grow nanohelices, and here we briefly review the technical advances that are needed to grow complex shaped nanoparticles. The microstructures can be actuated by a magnetic field and possible applications of the micro- and nanohelices are briefly discussed. We also present a system of polymeric micro-screws that can be produced by micro-injection molding and that can be wirelessly driven by an external rotating magnetic field through biological phantoms, such as agarose gels with speeds of ~200 μm/s. The molding technique faithfully reproduces features down to a few microns. These microdrills can serve as a model system to study minimally invasive surgical procedures, and they serve as an efficient propeller for wireless microrobots in complex fluids. The fabrication scheme may readily be extended to include medically approved polymers and polymeric drug carriers.

Keywords: low Reynolds number propulsion, microrobot, microdrill, microscrew, glancing angle deposition, micro molding, biological tissue

1 INTRODUCTION

Moving through fluid environments at the scale of microorganisms presents a different set of challenges compared to those encountered by macroscopic swimmers. Particularly at low Reynolds number (Re << 1), which indicates a Stokes regime of fluid flow with a dominance of viscous forces over inertial forces, it is known that a simple time reversible motion will not result in any net displacement of the swimmer [1]. Hence, asymmetric non-reciprocal actuation mechanisms are required at low Re. Microorganisms use two non-reciprocal propulsion mechanisms: the travelling wave beats of cilia and the helical rotation of flagella.

Mimicking a rotating flagellum requires a rotary motor and power source capable of producing sufficient torque to overcome the high viscous drag at low Reynolds number. One may consider the use of electromagnetic motors, which are ubiquitous in macro-scale robotics. However, electromagnetic motors require sizeable currents which preclude miniaturization. One of the smallest commercial electromagnetic motors is 6 mm long with a diameter of 1.9 mm [2]. This is too large for applications in micro-surgery. Piezoelectric rotary motors do not require large currents and piezoelectric elements can readily be obtained that have small linear dimensions (~250 μm), but they require relatively high input voltages ~28 V_{pp} [3]. If the motor is to be powered wirelessly using a battery, then this presents a problem, as thin film lithium ion batteries typically supply microampere currents at 1-3 V which corresponds to μW (for an area of ~20 mm^2). Similarly, microfuel cells would require at least 1 cm^2 area of each electrode to produce power in the range of mW [4]. There are therefore no simple compatible combinations of motor and onboard powering source for designing sub-millimeter micro-swimmers. Hence, we resort to external magnetic fields and torques. Magnetically actuated rotation can be achieved with micro- and nanostructures that contain a ferromagnetic material and that can be actuated by a homogenous magnetic (*i.e.* gradient-free) field. However, in order for a robot to be propelled by a gradient-free field at low Reynolds number an asymmetrical shape is essential. Propulsion in this regime has been achieved with rigid chiral nanostructures, *i.e.* solid helically-shaped micro-propellers [5, 6]. A helix breaks spatial symmetry in a manner that allows for low Reynolds number propulsion by coupling rotational and translational motion; as a helical micro-robot rotates about its long axis, this hydrodynamic coupling leads to propulsion along this axis. Various fabrication techniques exist for constructing helical micro-robots:

1. 20 nm – 300 nm: Micellar nanolithography and shadow deposition (Glancing angle deposition) on cooled substrates [7]
2. 300 nm – 10 μm: Glancing angle deposition [5]
3. 10 μm – 100 μm: Direct laser writing of helical structures [8]
4. 20 μm – 100 μm: Metallic thin film strain engineering techniques [6]
5. 100 μm – mm: Micro molding [this work]

Here, we review the fabrication scheme and principle of operation of the smallest magnetically actuated microbots that can currently be operated in liquids (1 and 2, above). We also present a low-cost bench-top micro-molding scheme that is able to

produce polymeric magnetic micro-screws that can move in tissue phantoms (5, above). The choice of materials can thus be extended to medically approved polymers. Numerous applications can be proposed for the microbots at nano to micro length scales (1 and 2, above) especially in biological studies, *e.g.* as rheological probes to study the micro-rheology of complex biological media including cell membranes or as a carrier into the cell for genetic transfer; while the polymeric magnetic micro-screws (5, above) may serve as a micro-tool for biopsy in minimally invasive surgical procedures or as a vehicle for drug delivery.

2 FABRICATION OF NANOHELICES AND THE SMALLEST MICROBOTS

The fabrication technique that we focus on here is called glancing angle deposition (GLAD). With this method, a wide range of materials possessing many functionalities, such as ferromagnetism and electrical conductivity just to name a few, can be grown by physical vapor deposition, including magnetically-driven micro-robots [5]. The structures can be fabricated in large-numbers and with precisely defined geometries. This permits different length scales as well as different geometries to be realized that optimize the propulsive behavior at small scales [9].

GLAD is a physical vapor deposition technique [10-12]. A basic schematic is shown in Figure 1 (a). In a vacuum chamber at pressures of ~10^{-7} mbar, the source material is heated via electron beam bombardment until the material vaporizes. In the figure the vapor flux is for simplicity shown as a cone, but the vapor flux in general spreads with a broader angular distribution. Because of the low vacuum environment, the atoms impinge upon the substrate in a ballistic manner which is essential for taking advantage of the shadowing effect. Shadowing growth occurs when a surface onto which material is being deposited is tilted to a very oblique angle α, *i.e.* oblique angle deposition (OAD), which is typically $80° < \alpha < 87°$. Consider a substrate that is oriented at such an oblique angle. As the impinging vapor flux deposits on the substrate, if there is any surface roughness, *i.e.* raised portions of the substrate, the depositing material will preferentially accumulate on these raised features leaving the shadowed areas mostly free of material. If the substrate is perfectly flat, random nucleation sites will naturally form and serve as points of growth, but no regular ordering will be present in this case. If the substrate is intentionally seeded with well-ordered seeds, then the growth can be restricted to accumulate on the seed particles as will be discussed below.

The substrate, as shown in Figure 1 (a), is manipulated by two motors: the first motor, which is not shown in Figure 1, controls the vapor deposition angle α, which is defined as the angle between the flux and the substrate surface normal; the second motor controls the substrate rotation angle φ. No rotation of φ during deposition leads to arrays of nanorods tilted toward the plane of the substrate at an angle $\beta \neq \alpha$, whereas rapid rotation leads to growth of arrays of nanorods perpendicular to the surface. If the rotation is carefully controlled at intermediate speeds and in accordance with the rate of material deposition, an array of helices is produced. The helix pitch is inverse-

ly proportional to the rotation rate $d\varphi/dt$. It should be noted that the final morphologies are material-dependent and must therefore be tuned accordingly. For example, the substrate must be cooled significantly for materials with high adatom surface mobilities [7]. Multiple materials can be added subsequently for layered architectures or at the same time to produce various alloys. The three parameters that are used to characterize the morphology of an individual helix are presented in Figure 1 (b): *P* is the helix pitch, *R* is the helix major radius, and *r* is the helix minor, or wire radius. It should also be noted that there is a linear dependence upon the helix major radius and the helix pitch, but this is beyond the scope of the present article. Each parameter can be controlled to varying degrees as discussed below.

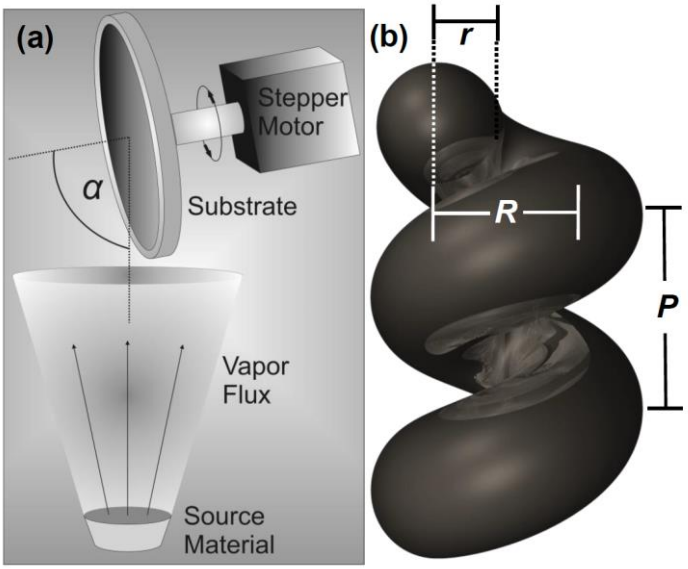

Fig. 1. (a) schematic of the GLAD process showing the source, vapor flux, and the orientation of the substrate; (b) schematic of an individual helix showing the helix minor radius *r*, helix major radius, *R*, and the helix pitch, *P*.

The morphology of the helix can be controlled in the following ways: the size of the initial seeds onto which the helix is grown translates directly to the size of *r* and defines the range of possible *P*; the substrate rotation rate $d\varphi/dt$ defines *P*; and the material which is being deposited.

Although a wide range of sizes can be fabricated with GLAD onto a non-patterned surface, in order to have greater control over the final morphology of the helix, and to have uniformity between helices in the helix array, a properly seeded substrate should be used. Electron beam (ebeam) lithography [13] is excellent for designing seed patterns, but if rapid fabrication is required, one must use a rapid seeding technique because e-beam lithography is slow and can only cover small areas. Here we describe methods to rapidly seed the substrates with individual seed dimensions ranging from several microns to nanometers. In this manner we can reproducibly construct helical

micro- and nano-robots over the entire wafer for over three orders of magnitude: from tens of nanometers to roughly ten microns.

The first technique requires patterning the wafer with an array of hexagonally close-packed spherical silica particles. This is accomplished using a Langmuir-Blodgett trough [14, 15]. As can be seen in Figure 2 (a), the ~ 400 nm SiO_2 beads are arranged in a close-packed arrangement on the surface of the substrate. It should be noted that defects in the monolayer crystal are present, but these are not important for our purposes here. For larger helices such as the 2-turn SiO_2 array shown in the cross-section SEM image in Figure 2 (b), this seeding approach is appropriate. These helices are then removed from the surface via sonication and suspended into a liquid, e.g. water. Individual helices which have been redeposited onto a new substrate for imaging are shown in the SEM image of Figure 2 (c) with a close up of a single helix in Figure 2 (d). This SiO_2 helix has a pitch P ~ 500 nm. The material is changed during growth and a magnetic material, Ni or Co, is sputtered onto the helices as shown in Figure 2 (c)-(d) [5]. The magnetic material is deposited at $\alpha = 0°$ and so coats only the top half. The helices are then magnetized in a manner that the magnetization direction is perpendicular to the helix axis. An alternative method is to incorporate the magnetic material into the structure during deposition as shown in Figure 2 (e) [16]. Clear contrast of the 150 nm of Co layer can be seen in the cross-section SEM image just above the silica beads.

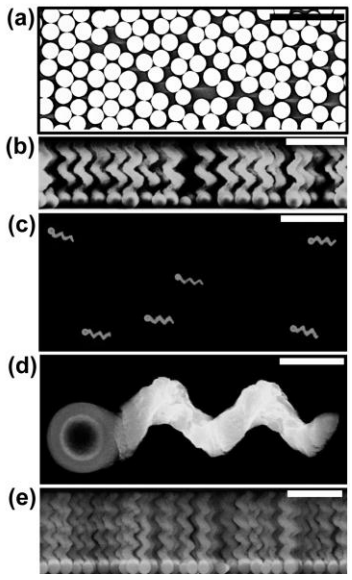

Fig. 2. (a) top-view SEM image of 400 nm SiO_2 beads on an Si(100) substrate; (b) side-view SEM of SiO_2 helices grown on the monolayer of beads; (c) individual helices removed from the array and redeposited onto another wafer; (d) a close-up of one of the same helices from (c); (e) a different 4-turn SiO_2 helix with a 150 nm layer of Co to add magnetic functionality as seen as the bright contrast just above the beads. Scale bar: (a), (b), (c), (d), and (e): 2 μm, 2 μm, 5 μm, 500 nm, and 2 μm respectively.

In order to produce nano-scale helices rapidly at the wafer-scale, we use the nano-lithography process called block co-polymer micellar lithography (BCML) [17] to seed the substrate. BCML requires the self-assembly of polystyrene-b-poly[2-vinylpyridine ($HAuCl_4$)] diblock copolymer micelles. Plasma treatment removes the polymer and reduces the Au-salt leaving behind hexagonally-arranged Au nanodots as shown in the top-view SEM image of Figure 3(a). The BCML process allows for the separation between seeds and the size of the individual dots to be tuned. We have recently shown that using the combination of BCML and GLAD allows for the fabrication of nano-colloidal particles with tailored optical, electromagnetic, and mechanical properties [7]. An example oblique angle SEM image of Cu nanohelices is shown in Figure 3 (b) and a TEM of an individual Cu helix is shown in Figure 3 (c). We reduce the temperature of the substrate before and during deposition to aid the shadowing effect and to reduce adatom mobility which is a key to the fabrication of helices of this size. The minor radius, r, for these Cu helices is < 20 nm with the overall length ~ 150 nm. This advanced fabrication technique allows for the fabrication of magnetic nano-scale helices as well, although nano-propulsion with helices of this size has yet to be demonstrated.

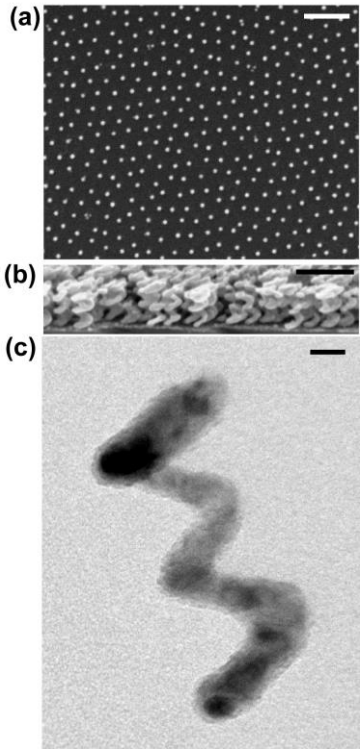

Fig. 3. (a) SEM top-view of a Si(100) wafer patterned via BCML nanolithography; (b) oblique-view SEM of 2.5-turn Cu helices grown on the BCML-patterned wafer; (c) TEM image of an individual Cu helix showing nanometer dimensions. Scale bar: (a), (b) 200 nm; and (c) 20 nm.

3 MAGNETICALLY ACTUATED MICROROBOTS

The micron-sized helices described in the previous section can be diametrically magnetized by a strong magnet. A (weak) rotating homogeneous magnetic field *B* can now be used to couple to the magnetic moment of the helices and this causes a rotation of the helices around the long axis, which, due to the symmetry-breaking of their chiral structure, leads to rotation-translation-coupling and therefore to a forward propulsion [5]. In our setup we use 3-axis Helmholtz coils that can generate rotating magnetic fields in 3D of more than 100 Gauss from DC to higher than kilohertz frequency by integration of an active water-cooling system into the metal frame of the coil [16]. A drawing of the coil's frame and a picture of an assembled Helmholtz coil system in an inverted microscope are shown in Figure 4. The field direction and strength is controlled with a custom LabView program, which enables us to steer the micro-propellers in 3D on micron-length scale.

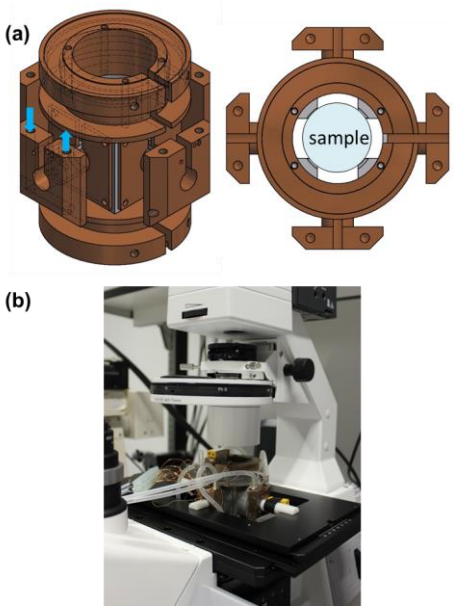

Fig. 4. (a) CAD drawing of the coil's frame (side and top view). The blue arrows indicate a water in-/outlet. (b) Image of the coil in an inverted microscope setup.

The propellers follow the magnetic field until the torque due to the applied magnetic field can no longer overcome the fluid's drag forces. This is called the step-out frequency. The translational speed of the helix depends linearly on the field's frequency

up to the step-out frequency and can be described by the following general analytical equation which we have derived in [16]:

$$v = \varepsilon\,\Omega = \varepsilon\left(\omega - \frac{\kappa \quad \sec^2\left[-\frac{t}{2C}\sqrt{\kappa} + \tan^{-1}\left[\frac{1}{\sqrt{\kappa}}\right]\right]}{C^2\omega\left(1 + \left(-\frac{1}{C\omega} + \frac{\sqrt{\kappa}}{C\omega}\tan\left[-\frac{t}{2C}\sqrt{\kappa} + \tan^{-1}\left[\frac{1}{\sqrt{\kappa}}\right]\right]\right)^2\right)}\right) \tag{1}$$

where

$$\kappa = C^2\omega^2 - 1 \tag{2}$$

and

$$C = \frac{X\,\eta}{M_{rem}\,B_0} \tag{3}$$

Here ω is the rotational frequency of the field and Ω is that of the particle, and t denotes time. The propeller's remanent magnetization is M_{rem}, the strength of the applied magnetic field is B_0 and η is the viscosity. X is a size-invariant geometry factor that depends only on the shape of the particle (for a sphere $X=8\pi$). The propulsion efficiency ε determines the forward translational speed at a given frequency and is a direct measure of the strength of the translation-rotation coupling. Its upper limit is set by the screw's pitch [16, 18]. For our GLAD structures, ε has a value on the order of a few nm/rad, and we can achieve speeds of about 2.5 μm/s at a magnetic field strength of 50 Gauss [16]. Figure 5 shows the velocities of the swimmers at various frequencies, as well as the trajectory of one microbot controlled by a joystick – demonstrating the control of the propulsion trajectory on micron-length scales.

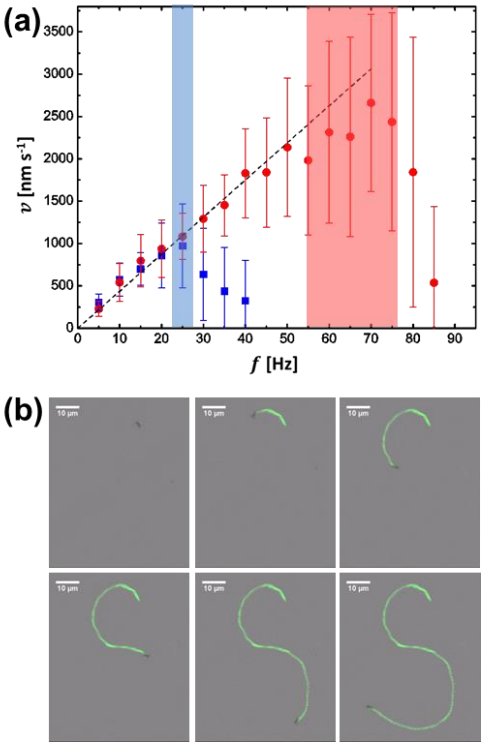

Fig. 5. (a) Propulsion speeds at various frequencies for magnetic field strengths of 20 and 50 Gauss (blue squares and red circles, respectively), with the step-out-frequencies indicated by the blue and red shaded areas (graph taken from Reference [16]), (b) trajectory of one actively driven micropropeller, demonstrating the control of the propulsion trajectory on micron-length scales.

The small size of these microswimmers combined with the high accuracy with which they can be propelled make them promising candidates for manipulation of biological systems on small length-scales. They are usually made out of silica, which can easily be functionalized with various chemicals, such as enzymes or fluorescent dyes. We therefore expect a number of interesting applications such as remote sensing and local micro-manipulation to emerge in the near future.

4 MICRODRILLS FOR BIOLOGICAL ENVIRONMENTS

At larger length-scales we use a metal micro-screw as a template from which we mold polymeric microdrills. The template is prepared by electrical discharge machining (EDM). As shown in Figure 6, the drill is designed to have an outer diameter of 300 µm in order to fit inside a 23 gauge needle (nominal inner diameter 337 µm). Hard-

ened steel is used as the template. The EDM process is time-consuming and is limited to conducting materials, which may not be suitable for medical applications. We have therefore developed a micro-molding process that uses a single EDM machined template from which polymer micro-screws may be batch-produced.

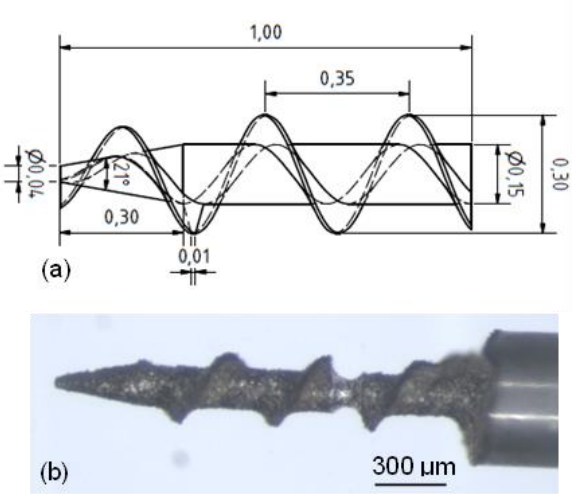

Fig. 6. The metal template for the micro-molding process. (a) Schematic drawing of the micro-screw design. Sizes are in mm. (b) Scanning electron microscope image of the micro-screw template manufactured by electro-discharge machining (EDM).

The micro-molding process consists of 6 steps, as illustrated in Figure 7. First, the metal template is manufactured by an EDM process (Institut für Mikrotechnik in Mainz, Germany (Figure 7 (a)). Then Polyvinyl siloxane (PVS) impression material (Art. No 4667, Coltene Whaledent, Switzerland) is mixed and the metal template is inserted (Figure 7 (b)). After 5 min curing, the metal template is removed (Figure 7 (c)). Cycloaliphatic Epoxide Resin (ERL-4221 Modified SPURR Embedding Kit, SERVA Electrophoresis GmbH, Heidelberg, Germany) is then injected into the mold (Figure 7 (d)). After the epoxy is cured at 70°C for 3 hours, the PVS mold is cut and split, and the polymer micro-screw is released (Figure 7 (e)). Finally, a cylindrical NdFeB micro-magnet (200 µm in diameter and 400 µm in length) is attached to the end of the polymer (Figure 7 (f)). By this cheap and fast micro-molding process, the micro-structure of the metal template is precisely replicated.

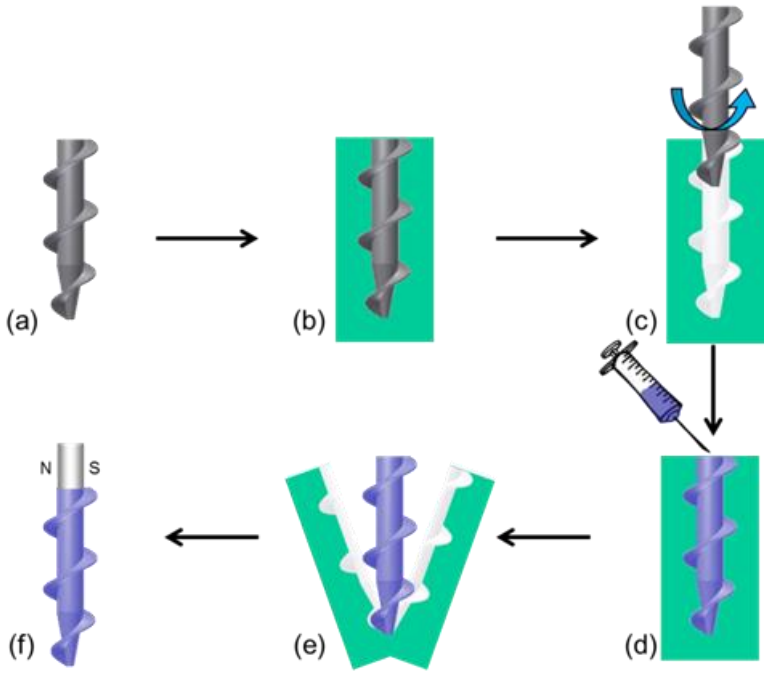

Fig. 7. Illustration of the micro-molding process. (a) Metal template by EDM. (b) Micro-molding using PVS. (c) After curing of the PVS mold, removal of the metal template. (d) Polymer injection and curing. (e) Unmolding by splitting the PVS mold. (f) Magnet attachment.

To test the magnetic micro-screw, we have used a tri-axial Helmholtz coil (similar to the one discussed in section 3). The coil can generate fields of up to 80 Gauss at up to 100 Hz (Figure 8). We use custom LabView software to control the amplitude and direction of the rotating magnetic field in 3D. To mimic the rheological properties of biological tissue we prepare various agarose gels for *in vitro* testing. Figure 9 shows a micro-screw that is propelled in agarose gels. We have tried propulsion in 0.1% wt-1% wt agarose gels, the latter requiring higher fields (up to 500 Gauss). The trajectory (see Figure 9 (d)) is defined in real time by a joystick. The average linear velocity reaches roughly 200 μm/s with a magnetic field rotating at 5 Hz.

Fig. 8. Helmholtz coil setup to drive the micro-screw. (a) Tri-axis Helmholtz coil setup is used to drive and steer the micro-screw. Stereo-microscope (Leica MZ95 stereoscope with a Leica DFC 490 camera) is used to observe the movement. (b) 3-dimensional navigation of the micro-screw can be realized by turning the magnetic field with a joystick. (c) Enlarged picture of the tri-axial Helmholtz coil.

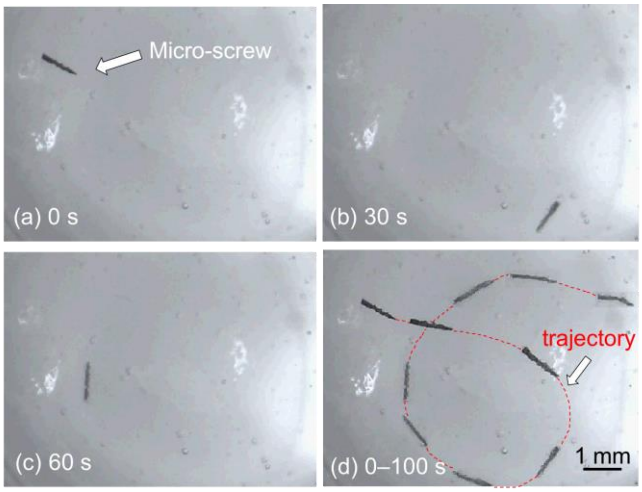

Fig. 9. Propulsion of the micro-screw in agarose gel. Snapshots after (a) 0 s, (b) 30 s, (c) 60 s, respectively, (d) the trajectory of the micro-screw from 0 to 100 s defined by the external magnetic field.

5 CONCLUSIONS

We have reviewed fabrication methods that can be used to grow some of the smallest magnetically actuated microrobots. We have shown how helical structures that are smaller than 100 nm can be made. We illustrated the excellent control that we have over material composition and shape that this fabrication scheme offers and the superior control that we obtain when actuating these structures in fluids. We have also demonstrated controlled magnetically-actuated propulsion of a polymer micro-screw in agarose gels. The fabrication is convenient and scalable and permits larger numbers of screws to be obtained quickly. The micro-molding process can serve as a cost-effective replication method for microbot propellers. The micro-screws have the potential to be used as an efficient propeller for self-powered wireless microbots in fluids. The systems may serve as promising micro-tools for minimally invasive therapeutics, and the fabrication scheme is general such that it permits the use of medically approved polymeric materials. Both schemes permit the use of surface chemistries or the loading with suitable molecules and drugs.

6 ACKNOWLEDGMENTS

The authors thank C. Miksch for helpful suggestions and for assistance with the micro-molding setup and B. Miksch for assistance with the LabView program. This work was supported by the European Research Council under the ERC Grant agreement Chiral MicroBots (278213).

REFERENCES

1. Purcell, E. M.: Life at Low Reynolds-Number. Am J Phys. 45, 3-11 (1977)
2. http://www.micromo.com/datasheets/BrushlessDCmotors/0206_B_DFF.pdf.
3. Watson, B., Friend, J., Yeo, L.: Piezoelectric ultrasonic resonant motor with stator diameter less than 250 μm: the Proteus motor. J Micromech Microeng. 19, 022001 (2009)
4. Cook-Chennault, K. A., Thambi, N., Sastry, A. M.: Powering MEMS portable devices - a review of non-regenerative and regenerative power supply systems with special emphasis on piezoelectric energy harvesting systems. Smart Mater. Struct. 17, 043001 (2008)
5. Ghosh, A., Fischer, P.: Controlled Propulsion of Artificial Magnetic Nanostructured Propellers. Nano Letters. 9, 2243-2245 (2009)
6. Zhang, L., Abbott, J. J., Dong, L. X., Kratochvil, B. E., Bell, D., Nelson, B. J.: Artificial bacterial flagella: Fabrication and magnetic control. Applied Physics Letters. 94, 064107 (2009)
7. Mark, A. G., Gibbs, J. G., Lee, T.-C., Fischer, P.: Hybrid nanocolloids with programmed 3D-shape and material composition. Nature Materials. 12, 802-807 (2013)
8. Tottori, S., Zhang, L., Qiu, F. M., Krawczyk, K. K., Franco-Obregon, A., Nelson, B. J.: Magnetic Helical Micromachines: Fabrication, Controlled Swimming, and Cargo Transport. Adv Mater. 24, 811-816 (2012)

9. Keaveny, E. E., Walker, S. W., Shelley, M. J.: Optimization of Chiral Structures for Microscale Propulsion. Nano Letters. 13, 531-537 (2013)
10. Hawkeye, M. M., Brett, M. J.: Glancing angle deposition: Fabrication, properties, and applications of micro- and nanostructured thin films. Journal of Vacuum Science & Technology A: Vacuum, Surfaces, and Films. 25, 1317-1335 (2007)
11. Robbie, K., Brett, M. J.: Sculptured thin films and glancing angle deposition: Growth mechanics and applications. 15, 1460-1465 (1997)
12. Zhao, Y. P., Ye, D. X., Wang, G. C., Lu, T. M.: Novel Nano-Column and Nano-Flower Arrays by Glancing Angle Deposition. Nano Letters. 2, 351-354 (2002)
13. Dick, B., Brett, M. J., Smy, T.: Controlled growth of periodic pillars by glancing angle deposition. Journal of Vacuum Science & Technology B: Microelectronics and Nanometer Structures. 21, 23-28 (2003)
14. Roberts, G.: Langmuir - Blodgett films. Plenum, New York (1990)
15. Reculusa, S., Ravaine, S.: Synthesis of colloidal crystals of controllable thickness through the Langmuir-Blodgett technique. Chem Mater. 15, 598-605 (2003)
16. Schamel, D., Pfeifer, M., Gibbs, J. G., Miksch, B., Mark, A., Fischer, P.: Chiral Colloidal Molecules And Observation of The Propeller Effect. Journal of the American Chemical Society. 135, 12353-12359 (2013)
17. Glass, R., Moller, M., Spatz, J. P.: Block copolymer micelle nanolithography. Nanotechnology. 14, 1153-1160 (2003)
18. Baranova, N. B., Zeldovich, B. Y.: Separation of Mirror Isomeric Molecules by Radio-Frequency Electric-Field of Rotating Polarization. Chem Phys Lett. 57, 435-437 (1978)